A modified model for dynamic properties of visual receptive field*

CHEN Yuzhi (陈育志)**, WANG Yunjiu (汪云九) and QI Xianglin (齐翔林)

(Laboratory of Visual Information Processing, Institute of Biophysics, Chinese Academy of Sciences, Beijing 100101, China)

Received August 19, 1999; revised September 6, 1999

Abstract The extended Gabor function model for visual receptive field (RF) was modified by substituting the term related to time with two-order integral kernel of Γ function to generate a new model called modified Gabor function model of RF. A set of the modified Gabor models (MGM) can present the major spatiotemporal properties of neuronal receptive fields at different levels of primary visual pathway. The transient responses, dynamic properties of RF simulated by MGM, are in good agreement with the observations in electrophysiological experiments.

Keywords: visual receptive field, dynamic property, mathematical model.

In the late 1980s, the development of receptive field (RF) mapping techniques using advanced computer and powerful mathematical tools (such as white-noise analysis) facilitated the study of dynamic properties of neuronal RF in visual pathway. By these techniques, a rapid and pseudo-random stimulus sequence consisting of patterns of light spots or bars can be presented. At the same time the neuronal spike train is found to be correlated to the stimulus sequence. Then the dynamic process of RF for a single cell can be calculated by means of correlation procedure, namely cross or reverse-correlation. Moreover, the changeable excitatory and inhibitory subregions of spatiotemporal RF can be demonstrated from the results of electrophysiological experiments, thus the entire RF can be presented more precisely. The dynamic RFs have been shown to exist in various cells of retina, lateral geniculate nucleus (LGN) and visual cortex of cat and monkey.

Three mathematical models related to the dynamic properties of receptive fields were proposed in 1985[1—4]. The first mathematical model for describing spatiotemporal RF was the extended Gabor function model (EGM) proposed by Wang et al. and Pan et al.[1,2]. The motion perception model in human vision was suggested by Watson and Ahumada based on Hilbert spatiotemporal filter[3], and it was only compared with the results of psychophysical experiments. Adelson and Bergan proposed the spatiotemporal energy model on motion perception[4]. In 1987 Heeger suggested another motion model that was the same as the EGM[5]. Grzywacz and Yuille explained the detection of motion velocity based on the Heeger's model[6]. Kawakami and Okamoto described the five kinds of cells in visual magno-system in terms of Haugh transform to explain the perception of moving image[7]. Wang et al. simulated the major dynamic characteristics of RF by the EGM in 1996[8]. In this study a modified Gabor function model is proposed, in which the EGM is modified in its temporal part, namely terms

* Project supported by the National Natural Science foundation of China (Grant No. 39893340-06, 69835002, 39670186).

** Present address: Center for Neurobiology & Behavior, Columbia University, 722 W, 168th St., New York, NY 10032, USA.

related to time are substituted by two-order integral kernel of Γ function. And its spatial part remains the same as the original.

1 Description of the model

In the modified model, Gabor function is still adopted as the term related to spatial variables and the temporal term is substituted by two-order integral kernel function of Γ function $t^{z-1}e^{-t}$. When $z=2$, $t^{z-1}e^{-t}=te^{-t}$. Then the modified Gabor function model (MGM) is expressed as follows.

1.1 Isotropic MG model in polar coordinates (First type of MGM)

$$MG_1(r,\varphi,t) = K\cos(\omega_r r+\theta_r)\exp(-r^2/\sigma_r^2)\cos(\omega_t t+\theta_t)\cdot\frac{t}{T_1}\exp(-(t-\tau)/T_2)$$

$$= G(r,t)\frac{t}{T_1}\exp(-(t-\tau)/T_2), \tag{1}$$

where $G(r,t)=K\cos(\omega_r r+\theta_r)\exp(-r^2/\sigma_r^2)\cos(\omega_t t+\theta_t)$, r and φ are spatial polar coordinates, ω_r spatial frequency, ω_t temporal frequency, σ_r spatial variation, θ_r spatial phase and θ_t temporal phase, T_1, T_2, τ and K are constants.

1.2 Anisotropic MG model in Cartesian coordinates

(i) Spatiotemporal separable MG model (Second type of MGM)

$$MG_{21}(x,y,t) = K\cos(\omega_x x+\omega_y y+\theta_{xy})\exp(-x^2/\sigma_x^2-y^2/\sigma_y^2)\cos(\omega_t t+\theta_t)$$

$$\cdot\frac{t}{T_1}\exp(-(t-\tau)/T_2) = G(x,y,t)\cdot\frac{t}{T_1}\exp(-(t-\tau)/T_2), \tag{2}$$

where $G(x,y,t)=K\cos(\omega_x x+\omega_y y+\theta_{xy})\exp(-x^2/\sigma_x^2-y^2/\sigma_y^2)\cos(\omega_t t+\theta_t)$.

(ii) Spatiotemporal inseparable MG model (Third type of MGM)

$$MG_{22}(x,y,t) = K\cos(\omega_x x+\omega_y y+\omega_t t+\theta_{xyt})\exp(-x^2/\sigma_x^2-y^2/\sigma_y^2)\cdot\frac{t}{T_1}\exp(-(t-\tau)/T_2)$$

$$= G(x,y,t)\cdot\frac{t}{T_1}\exp(-(t-\tau)/T_2), \tag{3}$$

where $G(x,y,t)=K\cos(\omega_x x+\omega_y y+\omega_t t+\theta_{xyt})\exp(-x^2/\sigma_x^2-y^2/\sigma_y^2)$, x and y are spatial coordinates, ω_x and ω_y spatial frequencies, ω_t is temporal frequency, σ_x and σ_y are spatial variations, θ_{xy} is spatial phase, θ_t temporal phase, θ_{xyt} spatiotemporal phase and other symbols are the same as in equation(1).

2 Comparing the MG model with electrophysiological experiments

2.1 Transient responses of receptive field

DeAnglis reported two kinds of typical responses of simple cells in visual cortex to a sustained flash light bar in electrophysiological experiments[9]. One is the transient response of a cell with space-time inseparable RF (fig.1(a)), and the other is the response with space-time separable RF (fig.1(b)). The left panels of figs.1(a) and (b) are the $x-t$ profiles of RF. The ordinate indicates position x and its abscissa time t. The dotted lines in iso-amplitude contour maps represent the inhibitory subregions with different intensities and the solid lines the excitatory subregions with different intensities. The $x-t$ plot in fig.1(a) exhibits bright- and dark-excitatory subregions that are tilted in the space-time domain because this kind of RF is spatiotemporal inseparable. While in the $x-t$ plot of fig.1(b) the boundary between the excitatory area and inhibitory area is parallel to the abscissa, indicating the RF map is separable in space-time domain. The right panels of figs.1(a) and (b) demonstrate the responses of a simple cell to sustained flash of a light bar stimulus at different positions of RF. The cell gives an "ON" response at positions 1 and 3 and an "OFF" response at position 2 (fig.1(a)). In fig.1(b), the cell has a sustained "ON" response at position 1, and the "OFF" response at position 2 was observed. So ON/OFF map can be derived from the $x-t$ profiles, the ON/OFF description is not completed alone.

When the parameters are chosen properly in formulas of MG_{21} and MG_{22}, the simulated results can be in good agreement with the experimental results. Figs.1(c) and (d) are the simulated results obtained from MG_{21} and MG_{22} respectively. The left panel of fig.1(c) presents the excitatory and inhibitory subregions with multiple lobes, which are similar to that in fig.1(a). In fig.1(d), there is a clear boundary between the regions, and is parallel to the abscissa. The simulated results in figs.1(c) and (d) conform qualitatively with the experimental results obtained by electrophysiological record shown in fig.1(a) and (b). The "ON" response appears at positions 1, 3 and "OFF" at position 2 in the right panel of fig.1(c), but the "ON" occurs at position 1 and "OFF" at position 2 in fig.1(d). Thus it can be seen that both the spatiotemporal separable and inseparable models of MG are qualitatively agreeable to the transient responses of simple cells to a light spot or bar.

2.2 Simulating the dynamics of simple cells in visual cortex

In the late 1980s, the development of powerful RF mapping technique promoted the studies on the dynamics of RF in physiology. A series of "snapshots" of dynamic RF can be obtained by means of a reverse correlation technique. The typical spatiotemporal distributions on $(x-y-t)$ for representative simple cells of cat's striate cortex are shown in figs. 2(a) and (b). The $x-y$ plots indicating the 2-D spatial profiles at different time are shown as iso-amplitude contour maps. The excitatory subregion is delimited by solid contour lines and the inhibitory by broken contour lines. Below these plots each 1-D profile of RF is obtained by integrating the 2-D profile along the y axis that parallels the preferred orientation of the simple cell. Fig. 2(a) illustrates that the spatial distribution of RF subregions is fixed but their strengths and polarities are modulated over time. The temporal sequences of RF profiles in fig. 2(b) look like a movie. The subregions of the RF in fig. 2(b) appear

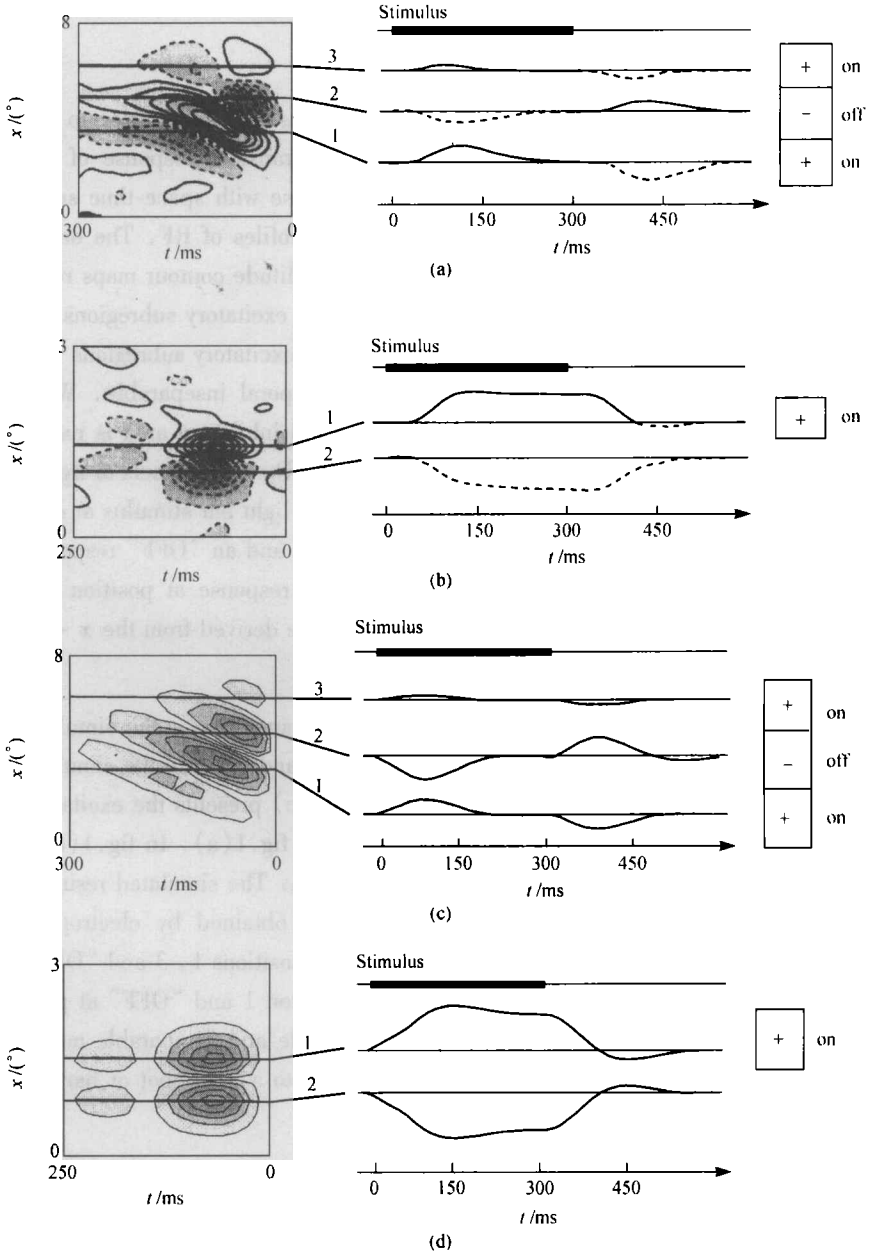

Fig. 1. Comparison of the simulation results of MG model with the responses of two simple cells to a sustained flash of a light bar. The left plots of (a) and (b) illustrate the spatio temporal iso-amplitude where the solid contours stand for excitation subregion and the broken contours for inhibition subregion[9]. The right panels of (a) and (b) indicate the transient response of the cell to a flashed bright bar at positions 1, 2 and 3. (The experimental results are quoted from ref. [9]). (c) Shows the simulated results by MG_{22}, the parameters are $\omega_x = 0.5\pi/\text{deg}$, $\sigma_x = 2$ deg, $\omega_t = -\pi/150$ ms, $\tau = 60$ ms, $\theta_{xyt} = -1.2\pi$. (d) shows the simulated results by MG_{21}, the parameters are $\omega_x = 0.5\pi/\text{deg}$, $\sigma_x = 0.5$ deg, $\omega_t = \pi/150$ ms, $\theta_{xy} = 0.5\pi$, $\tau = 50$ ms, $\theta_t = 0.5\pi$.

to move rightward along x axis over time within a spatial window. When the parameters were chosen properly, the spatiotemporal separable and inseparable RF were simulated by MG_{21} and MG_{22} respectively (figs.2(c) and (d)). In fig.2(c), the value of excitation rises with time first, then decreases afterward. But both the increase and decrease of the excitatory values can take place in the same position of RF. In fig.2(d) the excitatory values are increased at first and then decreased thereafter. It is observed that the excitatory area is drifted rightward in fig.2(d). In these aspects the simulations of

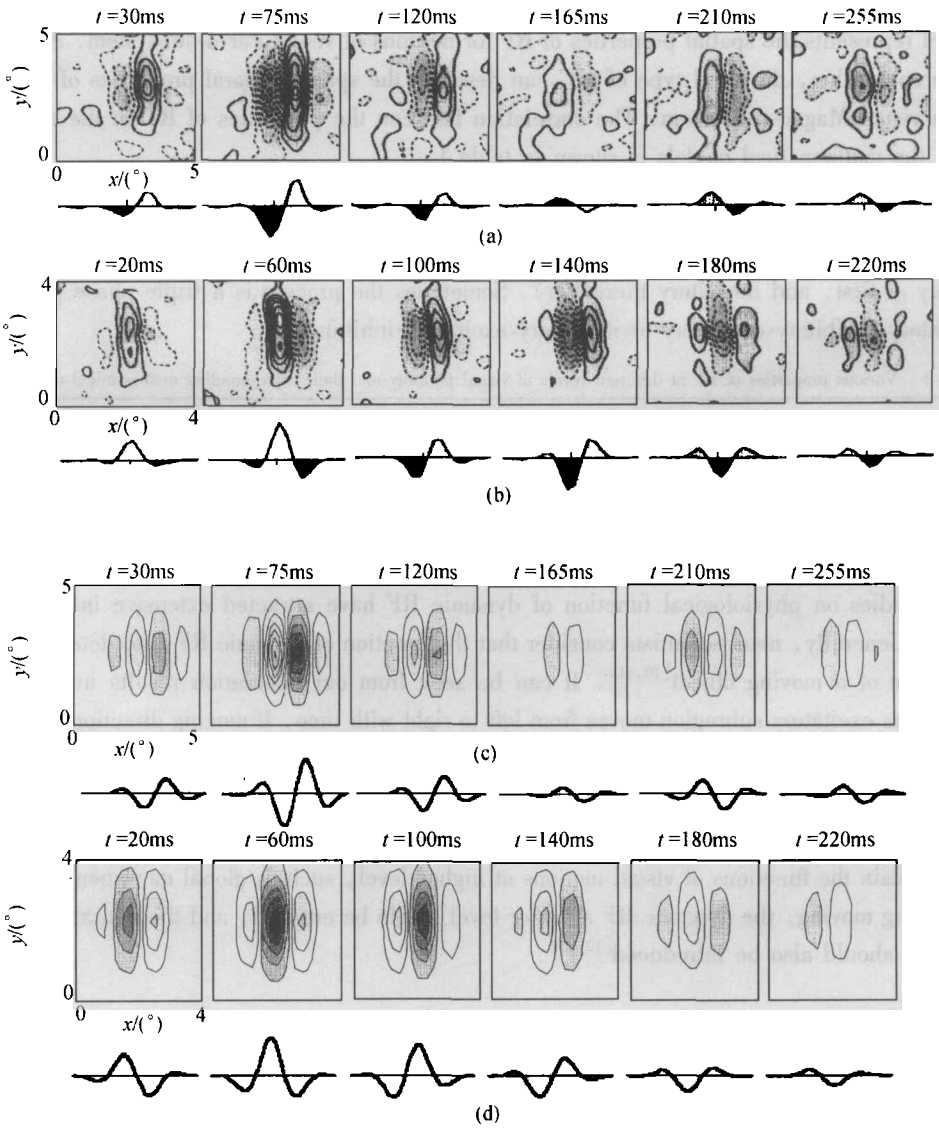

Fig. 2. Experimental and simulated results of the dynamics of receptive field structure of simple cells. The properties of spatiotemporal separable (a) and inseparable (b) RF respectively[9]; (c) The results simulated by MG_{21}, where $\omega_x = \pi/\text{deg}$, $\omega_y = 0\ \pi/\text{deg}$, $\sigma_x = 1.3$ deg, $\sigma_y = 1.3$ deg, $\omega_t = \pi/150$ ms, $\tau = 75$ ms, $\theta_{xy} = -0.45\pi$ and $\theta_t = -0.5\pi$; (d) the simulated results by MG_{21}, where $\omega_x = \pi/\text{deg}$, $\omega_y = 0\pi/\text{deg}$, $\sigma_x = 1$ deg, $\sigma_y = 1.2$deg, $\omega_t = -\pi/120$ ms, $\tau = 60$ ms and $\theta_{xy} = 0.6\pi$.

MG models are well consistent with the electrophysiological data.

3 Discussion

The spatiotemporal properties of isotropic RF for neurons from retina and LGN can be described by the first type of MGM. The second type and the third type of MG models can present the dynamic properties of anisotropic RF for neurons from visual cortex, while MG_{21} corresponds to spatiotemporal separable RF and MG_{22} to inseparable RF. If the temporal frequency ω_1 is zero, the second type of MG model represents the spatial properties of RF for neurons of visual Parvo-subsystem. And when ω_1 takes a proper value, the third type of MG can describe the spatiotemporal properties of RF for neurons from visual Magno-subsystem. The correlation between the properties of RF in the two sub-systems and the mathematical models is shown in table 1.

It is more reasonable that the temporal process is characterized by t times e^{-t}. When an initial stimulus is given, the response is zero, then it increases gradualy. It displays a two-phase process (excitatory at first, and inhibitory thereafter). Sometimes the process is a triple-phase process, that is, excitatory-inhibitory-excitatory or inhibitory-excitatory-inhibitory.

Table 1 Various properties of RF at different levels of visual pathway and their corresponding mathematical descriptions

Level of visual pathway	Spatial properties in Parvo-subsystem	Temporal properties in Magno-subsystem
Retina and LGN	$MG_1(r)$	$MG_1(r, t)$
Visual cortex	$MG_2(x, y)$	$MG_{21}(x, y, t)$ spatiotemporal separable $MG_{22}(x, y, t)$ spatiotemporal inseparable

The studies on physiological function of dynamic RF have attracted extensive interest from researchers. Generally, neuroscientists consider that the function of dynamic RF is to detect the velocity and direction of a moving object[10,11]. It can be seen from our simulation results in fig. 2(d) of MG_{22} that the excitatory subregion moves from left to right with time. If moving direction, velocity and spatial frequency of stimulus pattern are in accord with the properties of dynamic RF, the response of MG model can reach its maximum. Our study has demostrated that the key problem of detecting the direction of moving is the RF spatiotemporal inseparable neurons and their corresponding model. In order to explain the functions of visual motions at higher-level, such as global movement, aperture effect, masking moving, the dynamic RF at lower level has to be ensured, and the neural mechanism at higher level should also be introduced[12,13].

References

1 Wang, Y. J., Qi, X. L., Pan, Z. H., A mathematical model of primary information processing in vision system of vertebrate, Spatial properties of the model, *Acta Biophysica Sinica*, 1985, 1(2): 123.
2 Pan, Z. H., Qi, X. L., Wang, Y. J., A mathematical model of primary information processing in vision system of vertebrate. Temporal properties of the model, *Acta Biophysica Sinica*, 1985, 1(3): 189.
3 Watson, A. B., Ahumada, A. J., Model of human visual-motion sensing, *JOSA*, A, 1985, 2(2): 322.
4 Adelson, E. H., Bergen, J. R., Spatiotemporal energy models for the perception of motion, *JOSA*, A, 1985, 2(2): 284.
5 Heeger, D. J., Model for the extraction of image flow, *JOSA*, A, 1987, 4(8): 1455.
6 Grzywacz, N. M., Yuille, A. L., A model for the estimate of local image velocity by cells in the visual cortex, *Proc. R. Soc. Lond.*, B, 1990, 239: 129.

7 Kawakami, S., Okamoto, H., A cell model for the detection of local image motion on the magnocellular pathway of the visual cortex, *Vision Res.*, 1995, 36(1): 117.

8 Wang R., A network model for the optic flow computation of the MST neurons, *Neural Network*, 1996, 9(3): 411.

9 DeAngelis, G.C., Ohzawa, I., Freeman, R. D., Receptive-field dynamics in the central visual pathways, *TINS*, 1995, 18: 451.

10 Raab, M. J., Palmer, L. A., Contribution of linear mechanisms to the specification of local motion by simple cells in areas 17 and 18 of the cat, *Visual Neuroscience*, 1994, 22: 271.

11 Thompson, K. G., Zhou, Y. F., Leventhal, A. G., Direction-sensitive X and Y cells within the laminae of the cat's LGNd, *Visual Neuroscience*, 1994, 22: 927.

12 Nowlan, S. J., Sejnowski, T. J., A selection model for motion processing in area MT of primates, *The Journal of Neuroscience*, 1995, 15(2): 1195.

13 Wang, Y. J., Qi, X. L., Chen, Y. Z., Simulations of receptive-field dynamics, *TINS*, 1996, 19(9): 385.